ADVANCED SUSTAINABLE SYSTEMS
www.advsustainsys.com

Introducing Hydrogen Bond Networks in the Self-Assembly of Chitin Nanocrystals: Strong and Flexible Bioactive Films Containing Natural Polyphenols

Daniele Massari, Massimo Sgarzi, Matteo Gigli, and Claudia Crestini**

Free-standing, highly transparent and flexible films are obtained from solvent casting of aqueous colloidal dispersions of surface-deacetylated chitin nanocrystals. The Young's modulus and the water absorption of the films is further modulated by the addition of three natural polyphenols, i.e., epigallocatechingallate, tannic acid and one lignosulfonate, which differ one another in terms of molecular weight, and overall amount of hydroxy, phenolic and catecholic functionalities. The polyphenolic molecules create an extensive network of hydrogen bonds with the nanocrystals, thus controlling interfacial interactions. Therefore, they act as crosslinkers exerting a reinforcing and structuring action and hampering water absorption. The films do not show dissolution in water upon 7 days of incubation at room temperature, and the release profiles of the polyphenols in aqueous media evidence hindered Fickian diffusion kinetics confirming the presence of interactions with the nanostructured matrix. Lastly, the developed films possess bioactive properties, as they show both radical scavenging and antimicrobial activity. These characteristics are enhanced by the phenolic and, most importantly, catecholic moieties present in tannins (and to a lesser extent in lignins), allowing to reach bactericidal effects as high as 99.99% against both Gram-positive and Gram-negative strains.

1. Introduction

Finding innovative and robust solutions for the upcycling of biomass residues is of utmost importance to implement successful circular economy pathways. In particular, seafood waste represents an invaluable, yet underutilized source that, if effectively exploited, could significantly contribute to the production of a plethora of sustainable compounds and materials.[1] Estimations indicate that about 10 to 20 million tons of residues from fish industries are yearly generated.[2] In this scenario, the shellfish processing results in about 1.4 million tons dry weight of waste, of which up to 30% is chitin.[3] Chitin is indeed the second most abundant polysaccharide on Earth, as it constitutes one of the main components of the exoskeleton of insects and crustaceans, and it can be found also in the cell wall of fungi and microalgal species. Its backbone is composed by *N*-acetylglucosamine and glucosamine units randomly arranged along the macromolecular chains and linked by $\beta(1\rightarrow4)$ bonds. If the degree of acetylation (D_A) is higher than 0.5, the polymer is commonly defined as chitin, while for lower values as chitosan. Chitosan is thus the most important chitin derivative, and is obtained by simple deacetylation procedures.[4] Due to their large availability and relatively low costs, both chitin and chitosan have been extensively studied for decades, and their use in a wide range of applications ranging from food packaging to cosmetics, water treatment, biomedicine,[5] and, more recently, as electrochemical materials[6–8] has been tested. The high interest resides not only in the biobased nature, but also in the peculiar properties they show, such as biocompatibility, biodegradability, as well as antimicrobial, antioxidant, and antitumor activities.[9] Nevertheless, both chitin and chitosan display quite a number of drawbacks. Chitin is a high molecular weight, highly crystalline polymer, which exhibits insolubility in most organic solvents, hardness, and inelasticity.[10] Conversely, although its physical properties are strictly dependent on the molecular weight and D_A, chitosan is soluble in diluted organic and inorganic acid solutions at pH < 6, thus it can be more easily subjected to physical or chemical transformations than chitin.[11] However, the high hydrophilicity and pH sensitivity determine the low stability of chitosan-derived materials, e.g. films and fibers.

With the aim of overcoming the above-mentioned constraints, coupled with the exploitation possibilities opened by the nanoscale realm, chitin and chitosan nanomaterials, such as nanofibers and nanocrystals have attracted increasing attention.[12] Chitin nanostructures are more frequently synthesized by top-down approaches, as this avoids the use of harsh

D. Massari, M. Sgarzi, M. Gigli, C. Crestini
Department of Molecular Sciences and Nanosystems
Ca' Foscari University of Venice
Via Torino, 155, Mestre 30172, Italy
E-mail: matteo.gigli@unive.it; claudia.crestini@unive.it

The ORCID identification number(s) for the author(s) of this article can be found under https://doi.org/10.1002/adsu.202400389

DOI: 10.1002/adsu.202400389

conditions, and therefore could help preserving the structural characteristics of chitin, such as its crystalline domains.[13] Specifically, chitin nanocrystals (ChNCs) are prepared by acid hydrolysis of the amorphous regions, which results in the formation of high aspect-ratio crystalline structures.[14] The surface of ChNCs can be subsequently modified by post-functionalization strategies, e.g. alkaline treatment that yields surface-deacetylated chitin nanocrystals (CsNCs).[15]

ChNCs and CsNCs have been mainly used as reinforcing fillers in biopolymeric matrices,[16,17] while their self-assembly ability has been only very seldomly described.[18] Previous reports focus on the optimization of the conditions for the nanocrystals preparation,[18] or on the comparison of the tensile behavior of films originated by chitin nanocrystals and chitin nanofibers.[19] However, to be best of our knowledge, the functional properties of CsNCs films have never been studied, nor polyphenol-containing CsNCs films have been ever prepared before.

On the other hand, much research has been lately carried out to develop films based on cellulose nanocrystals (CNC) by exploiting the self-assembly ability of these nanostructures. A wide variety of components was added to the formulation with the aim of modulating the supramolecular structure and the optical, mechanical, and physical properties of the prepared materials in view of their potential application as multifunctional sensors. Furthermore, the use of natural polyphenolic moieties, particularly lignin, as functional additives was explored.

The introduction into CNC matrices of chitosan, deacetylated chitin nanofibers or lignin nanoparticles, which intercalated within the CNC nematic structure, permitted to modulate the size of their helical pitches and to increase the hydrophobicity of the films, finally achieving fast humidity and pH reversible responsiveness.[20,21] CNC was also combined with other polysaccharides such as arabinogalactan, galactomannan or konjac glucomannan, and low molecular weight compounds like tartaric acid and benzoic anhydride.[22,23] Antimicrobial, UV-shielding, and biocompatible membranes with high mechanical strength and toughness were thus prepared thanks to the extended network of hydrogen bonds assured by the different components. Lastly, adjustable optical properties and high UV-blocking capacity were very recently obtained in carboxymethylcellulose-derived films containing CNC and lignosulfonate.[24] These active components granted high transparency and haze, and improved tensile behavior with respect to pure carboxymethylcellulose films.

On these bases, it is herein hypothesized that the film-forming ability of CsNCs, integrated with the in situ generation of a network of hydrogen bonds induced by the presence of natural polyphenols, can be effectively exploited to generate bioactive free-standing films with specific and unprecedented properties.

To this aim, polyphenol-containing CsNCs films were prepared by solvent casting of aqueous colloidal dispersions. The main objectives of the work being: i) to modulate the films properties by studying the role of the hydrogen bond density and extension on the physic-mechanical and functional properties of the CsNCs-based films, and ii) to endow the films with strong antioxidant and antimicrobial capacity due to the synergistic action of the CsNCs-based matrix and the polyphenolic moieties.

More specifically, epigallocatechin gallate, tannic acid, and lignosulfonate were selected as examples of monomeric, oligomeric, and polymeric polyphenols, respectively displaying different amounts of phenolic and catecholic groups. Film color and transparency, surface hydrophilicity, and water absorption were evaluated, together with the tensile properties of the prepared materials. The release kinetics of the polyphenols from the CsNCs matrix and the release mechanism were studied and correlated with the antioxidant and antibacterial activity, the latter being assessed against both Gram-positive and Gram-negative strains.

2. Results and Discussion

2.1. Synthesis and Characterization of ChNCs and CsNCs

The preparation of ChNCs involves the hydrolysis of the chitin amorphous domains and the isolation of the crystalline fraction. A subsequent step of surface deacetylation yields the CsNCs. Prior to further analysis, ChNCs and CsNCs were stored in the form of never-dried gel, respectively having a concentration equal to 11.6 and 13.1 wt.%.

To verify the success of the deacetylation treatment, ChNCs, CsNCs, and pristine chitin were subjected to elemental analysis (CHNS). The results, reported in Table S1 (Supporting Information), demonstrate that the hydrolysis process of the amorphous part of the polymer did not lead to any variation in the N/C ratio. On the contrary, the subsequent deacetylation step resulted in the increase of the N/C ratio due to the removal of the $CH_3CO–$ groups. The collected data are in agreement with those reported in the literature.[25] CHNS data also evidence a greater concentration of sulfur in the chitin sample with respect to the nanocrystals. At the biological level, sulfur is present in the amino acids cysteine and methionine, constituents of various proteins. Since the chitin used in this study was extracted from the exoskeleton of shrimps, it can be hypothesized that the presence of sulfur is due to a small amount of protein residues. The decrease in the sulfur content observed in the ChNCs and CsNCs samples can therefore be ascribed to the hydrolytic treatment, where not only the removal of the amorphous fraction of chitin occurs, but also the depolymerization of the protein residues into amino acids that are subsequently separated during the washing cycles. Furthermore, CHNS analysis allowed for the determination of the degree of deacetylation in both the ChNCs and CsNCs, which resulted respectively equal to 4.59% and 81.8%, confirming the success of the surface deacetylation step.

FT-IR and TGA analysis were carried out to further characterize the prepared materials in terms of chemical structure and thermal stability. It can be observed that the FT-IR spectra of ChNCs and CsNCs do not significantly differ (**Figure 1A**), indicating, as previously reported,[15] that the surface deacetylation process does not induce modifications of the chemical structure. All the characteristic bands of α-chitin associated to the different functional groups are visible. Specifically, the bands relative to O—H stretching at 3445 cm^{-1}, N-H stretching at 3262 and 3105 cm^{-1}, C—H vibrations in 2950–2850 cm^{-1} range, the split bands at 1660 and 1628 cm^{-1} corresponding to the amide I region (C═O stretching) and at 1560 cm^{-1} relative to the amide II band (C—N—H stretching and N—H bending), and the C—N stretching at 1160 cm^{-1} can be clearly distinguished.[15,26]

As to the TGA curves (Figure S1, Supporting Information), the first weight loss step, up to about 100 °C, is due to the

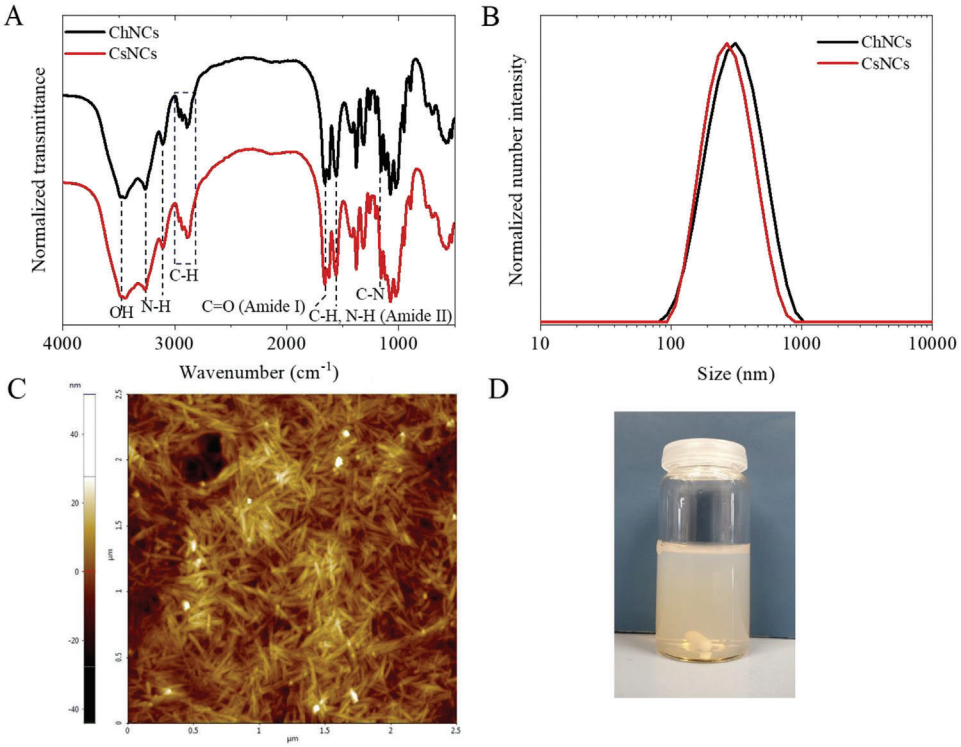

Figure 1. A) FT-IR spectra of ChNCs and CsNCs; B) number size distribution of ChNCs and CsNCs as measured by DLS; C) AFM micrograph of CsNCs; D) photograph of a 35 mg mL^{-1} colloidal suspension of CsNCs.

evaporation of residual water. Subsequently, up to 250 °C, no additional weight loss is observed, indicating the absence of any significant degradation paths for both samples. A second weight drop highlighted in the range of 250–400 °C can be attributed to the dehydration of the saccharide ring and to the decomposition of the acetylated and deacetylated units.[27,28] The weight loss observed at temperatures above 400 °C is finally linked to the complete decomposition of the polysaccharide residues.

To determine the size and morphology of the nanocrystals, DLS (Figure 1B) and AFM (Figure 1C) analyses were conducted. The typical rod-like shape of nanocrystals can be observed from the images collected via AFM. The tendency of the nanocrystals to aggregate in layered microstructures is also visible. The DLS analysis did not reveal huge size differences between the two samples, as ChNCs and CsNCs respectively showed a length of 350 ± 5 and 300 ± 3 nm, in agreement with previous studies.[29] To better evaluate the stability of the nanocrystals in the liquid formulation, zeta potential analysis was performed. ChNCs and CsNCs were dispersed in acidified water (pH 4.0) at a concentration of 1 mg mL^{-1} prior to the analysis. A value of +54.1 ± 0.7 and +55.4 ± 1.1 mV was recorded for ChNCs and CsNCs respectively, suggesting that stable colloidal suspensions can be prepared, as Z-potential values in the range between ±40 and ±60 mV usually indicate that aggregation and flocculation phenomena are prevented.[30] These data were supported by the observation that dispersions of CsNCs (Figure 1D) and ChNCs did not show any precipitate upon storage at room temperature for a period of at least 15 weeks.

2.2. Preparation of Free Standing CsNCs Films

The obtained nanocrystals were then used to prepare free-standing films via solvent-casting. Initially, to optimize the concentration of nanocrystals in the aqueous solution, films were fabricated dispersing CsNCs in water at pH 5.7. On the contrary, the use of ChNCs required a more acidic pH (4.0 or lower) to obtain stable dispersions. This result can be explained based on the repulsive stabilizing forces between the CsNCs with respect to the ChNCs, because the amino groups are readily protonated in acidic aqueous media.[31] A CsNCs concentration of 35 mg mL^{-1} was used, as lower concentrations caused either extended solvent evaporation times to gain films of comparable thickness or the generation of extremely thin films not suitable for proper handling, while concentrations above 40 mg mL^{-1} resulted in the formation of highly viscous gel-like dispersions with consequent casting difficulties. Depending on the concentration, ChNCs behave differently in aqueous suspension, forming isotropic, anisotropic nematic mesophase, and biphasic domains coexisting at intermediate concentrations.[32] The minimum concentration at which the formation of the liquid crystalline order occurs has been reported as high as 3.5 wt.%, although this value may slightly change depending on the specific morphology of the nanocrystals.[32] To further modulate the mechanical characteristics of the CsNCs film, glycerol was added as a plasticizer, as previously reported for CNC-based films.[33] Its introduction in the formulation was demonstrated to modify the film behavior from brittle to plastic, by decreasing the elastic modulus (E) of about one order of magnitude and improving

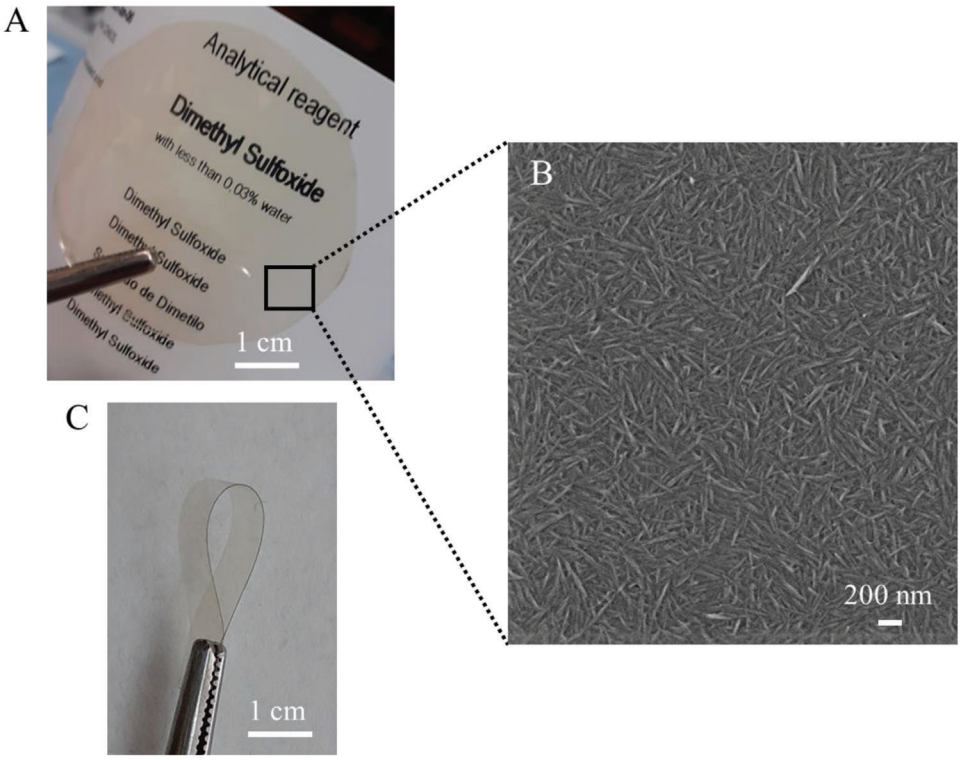

Figure 2. A) CsNCs-G film; C) SEM micrograph of the surface of a CsNCs-G film; C) bent CsNCs-G film.

the elongation at break (ϵ_b) up to 2.5-folds. The addition of glycerol was thus aimed both at increasing the flexibility of the matrix and at counteracting the stiffening effect provided by the presence of polyphenols, which can also form non-covalent interactions with the nanocrystals. Specifically, a concentration of glycerol equal to 30 wt.% with respect to the amount of CsNCs was used to produce CsNCs-G films (**Figure 2**). Figure 2B and Figure S2 (Supporting Information) show SEM micrographs of the film surface, where the CsNCs are clearly visible, and of its cross-section, which highlights the layering of the CsNCs.

2.3. Preparation of Polyphenol-Containing CsNCs Films, and Assessment of the Physic-Mechanical Properties

Different additives were subsequently added to the formulation with the aim of tailoring the mechanical behavior and providing additional functional characteristics. Specifically, three different bioactive water-soluble polyphenolic compounds were selected, namely epigallocatechin gallate (EGCG), tannic acid (TAN), and the methanol insoluble fraction of hardwood lignosulphonate (MIHLS), respectively representing monomeric, oligomeric and polymeric polyphenolic structures. The use of different polyphenolic compounds allowed not only to impart or improve additional features, such as antimicrobial and antioxidant activity, but also to evaluate the effect of the concentration of phenolic hydroxyl groups and of the molecular weight on the characteristics of the films.

The film formulations are reported in Figure S3 (Supporting Information). In all cases, high transparency was preserved, although a slight increase in opacity (up to 2.36%) can be detected upon the addition of polyphenols (Table S2, Supporting Information). A general increase of b^* was observed for the CsNCs-E, CsNCs-T, and CsNCs-L films as compared to CsNCs-G, indicating greater yellowness. In addition, a shift toward higher redness was recorded for CsNCs-E (Table S2, Supporting Information). In terms of whiteness, values above 75% were measured in all cases, with CsNCs-L showing the greater L^* index, equal to 92%. Overall, this caused an enhancement of the ΔE in all the polyphenol-containing films, with lower variations from CsNCs-G for CsNCs-L, and higher in the case of CsNCs-E (Table S2, Supporting Information). The results here reported are in line with those previously described for lignosulfonate-containing carboxymethylcellulose films, which evidenced an increase of brown coloring upon the enhancement of the lignosulfonate concentration yet maintaining good transparency, as transmittances above 90.8% were reported at 550 nm.[24]

Subsequently, the films were characterized in terms of surface wettability and water absorption by water contact angle and gravimetric measurements, respectively. The results obtained are shown in **Figure 3**.

The introduction of polyphenols in the formulation caused a modification of the wettability with respect to the CsNCs-G sample. Specifically, a reduction of the WCA can be observed in the case of CsNCs-E and CsNCs-T samples, while a slight hydrophobicity increase was measured for the CsNCs-L film (Figure 3A). The results obtained can be directly correlated to the concentration of hydroxyl and carboxylic groups, as measured by ^{31}P-NMR (Table S3, Supporting Information): the higher the concentration of polar functional groups, the lower the contact angle. The

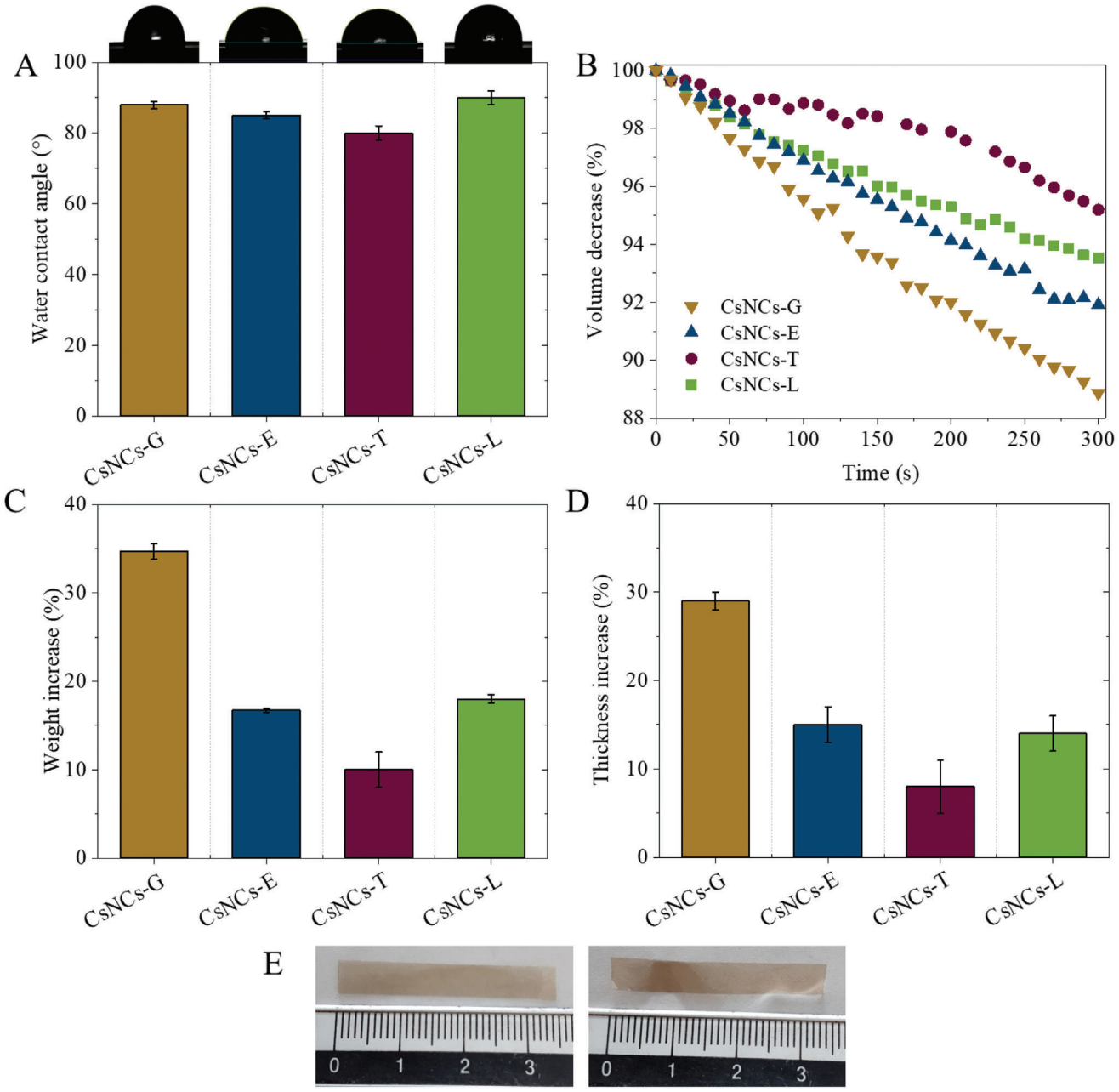

Figure 3. A) water contact angle of CsNCs-based films, top: water drops deposited on the film surface; B) variation of the volume of the water drop deposited on the film surface as a function of time; C) variation of the weight of CsNCs-based films due to water absorption after 10 min of incubation; D) variation of the thickness of CsNCs-based films due to water absorption after 10 min of incubation; E) photographs of a CsNCs-E film before (left) and after (right) incubation in water.

presence of sulfonate groups of MIHLS did not further increment the CsNCs-L surface wettability, rather, as previously demonstrated, the nonphenolic aromatic rings lowered the lignin-water interactions causing a hydrophobicity increase with respect to the other films.[21,34]

Furthermore, over the time frame of 5 mins, a decrease of the volume of the water drop deposited on the surface of the film was detected for all samples (Figure 3B). This phenomenon, due to the absorption of water within the film, depends on the formulation. Specifically, CsNCs-G showed a more significant decrease, while the polyphenol-containing samples exhibited a lower decrement.

As to the water absorption tests, the gravimetric measurements (Figure 3C) showed a weight increment of ca. 35% for the CsNCs-G sample. The introduction of polyphenols led to a much lower enhancement of the weight, as variations in the range of 9%–17% were recorded. The water absorption process reached equilibrium after 10 min, while a slight weight decrease over the

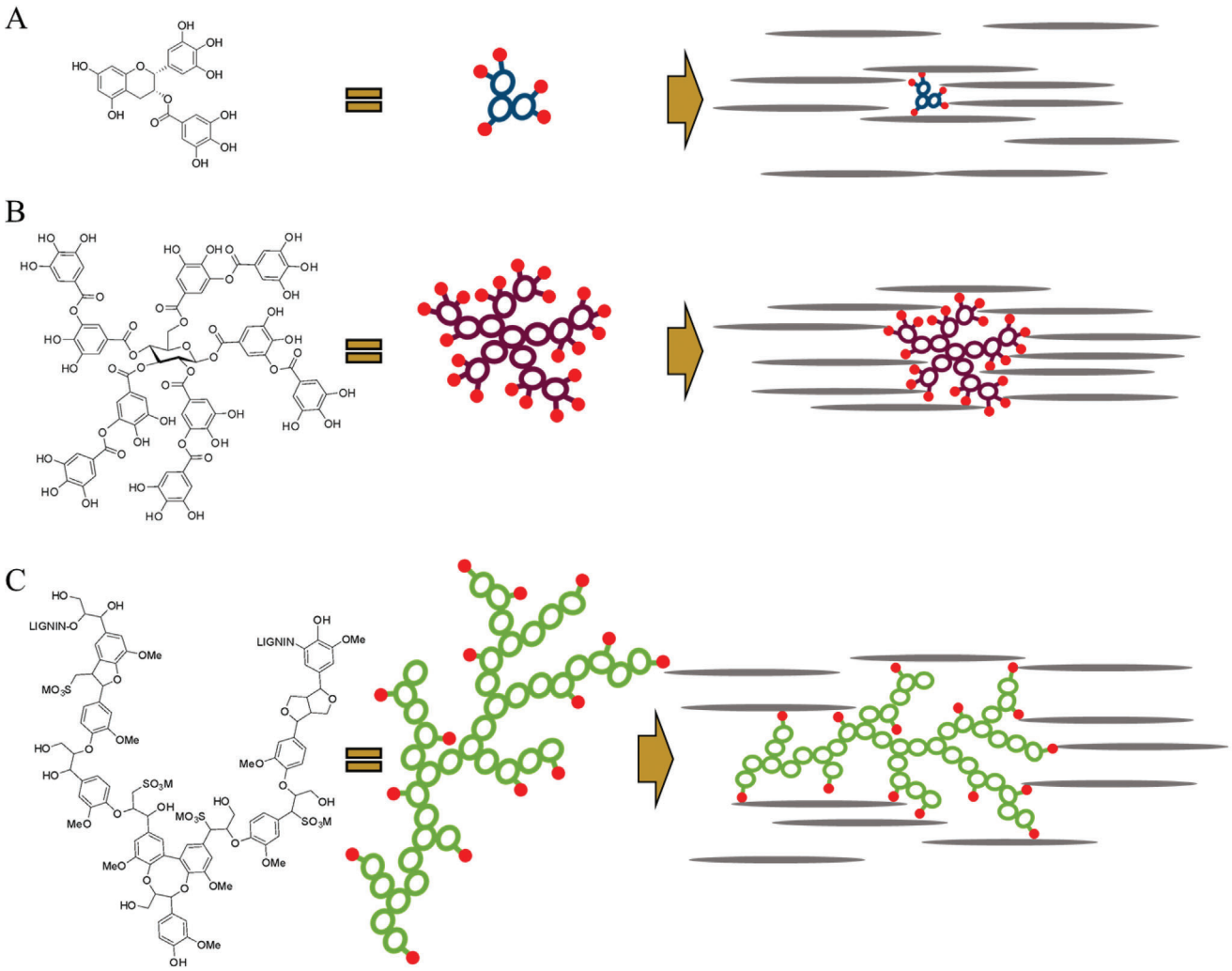

Figure 4. Cartoon showing the interactions of the different polyphenolic compounds with the CsNCs: A) EGCG; B) TAN; C) MIHLS.

course of 24 h was observed due to the diffusion of glycerol and polyphenols from the films to the aqueous medium (vide infra). It is worth mentioning that the CsNCs-based films, incubated in water up to 7 days at room temperature, did not show any dissolution, differently from polymeric chitosan.[35]

Similar findings were reported by Wang et al., who observed that an increasing amount of residual lignin in nanopaper had a positive impact on water absorption as a lowering of the water content was observed.[34] Of note, also in their case, a fast absorption over the course of 1 min was followed by a slower increase till saturation, reached in about 10 min.

After 10 min of incubation in water, length, width, and thickness of the films were measured and compared to the initial values. As can be seen from the data reported in Figure 3D,E, the film thickness significantly varies, while no appreciable changes in length and width are observed.

A lower increment of thickness was detected for the polyphenol-containing films with respect to the CsNCs-G sample, in agreement with the gravimetric measurements. Recent studies have demonstrated that ChNCs are arranged in stratified lamellae and that this arrangement is an intrinsic property of the nanocrystals.[36] On these bases, it can be hypothesized that water intercalates between the layers (the cross-section of a CsNCs-based film is reported in Figure S3, Supporting Information), leading to an increase of the thickness of the film. Previous studies indeed demonstrated that water molecules penetrate the chiral nematic structure of CNC films, increasing the helical pitch and, thus their thickness.[21]

Furthermore, the different behavior observed among the CsNCs-based films can be explained by considering the extension and overall amount of intermolecular hydrogen bonds established between the hydroxyl groups of the polyphenols and the hydroxy and amino groups of the nanocrystals (**Figure 4**).

A greater number of interactions keeps the film layers more closely linked to each other, thus hampering the swelling effect due to the intercalation of water molecules. This phenomenon is correlated to the peculiar chemical structure of the polyphenol introduced in the film and, specifically, to the density of hydroxy groups and to the molecular weight of the additive (Table S3, Supporting Information). The higher the concentration of OH

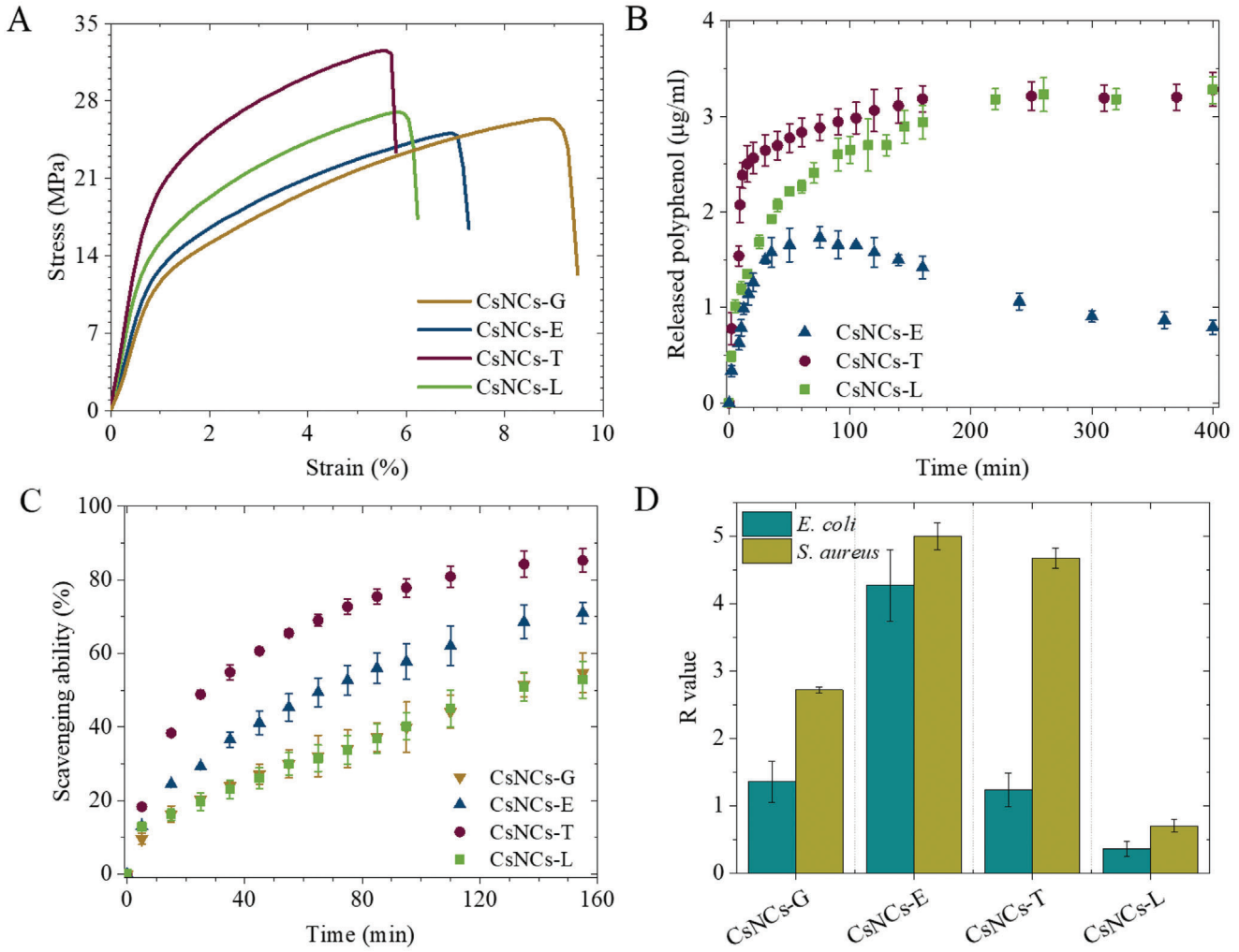

Figure 5. A) representative stress–strain curves; B) amount of polyphenols released in water as a function of time; C) antioxidant activity versus DPPH; D) antibacterial activity versus *E. coli* and *S. aureus*.

functionalities, the higher the amount of hydrogen bonds and relative crosslinks that can be formed.[37] Such cooperative hydrogen bonding, i.e., those generated by the presence of catechol moieties of polyphenols, can be only partially replaced by water molecules, while these last can more easily substitute glycerol. From this perspective, it can be also easily predicted that, whenever the overall cooperative hydrogen bond network increases in dimensions, the extent of water wettability and film thickness increase will be significantly reduced. The better results obtained using TAN as crosslinker over EGCG are readily rationalized just considering its higher molecular weight. Tannic acid can in fact assume different conformations thus easily adapting to optimize hydrogen bonding with the surface of the nanocrystals. In the case of lignosulfonate, despite its significantly higher hydrophobicity and molecular weight than TA, the low overall amount of aliphatic and phenolic groups results in a reduced capacity to prevent water adsorption with respect to tannic acid.

The tensile tests of the prepared films evidenced a clear dependence of the mechanical behavior on the characteristics of the polyphenol present in the formulation (**Figure** 5A; Table S4, Supporting Information) in agreement with the water absorption analysis.

Specifically, the presence of the polyphenolic moiety generates an enhancement of E. Of note, a more pronounced increase was recorded for the CsNCs-T sample, while comparable results could be observed for CsNCs-E and CsNCs-L (Table S4, Supporting Information). As to the stress at break (σ_b), CsNCs-T showed a greater value than the other samples, while in terms of strain at break a slight decrease was observed for all the polyphenol-containing films with respect to CsNCs-G. This behavior well correlates with the presence of multiple hydrogen bonds, as above described, which act as crosslinking points raising the film stiffness. The results here reported are in good agreement with literature data, since presence of additional compounds interacting with CNC, such as polysaccharides and functionalized polysaccharides, was proven to significantly impact the mechanical behavior of the films, by promoting higher flexibility and toughness.[22,23]

Subsequently, the release profile of the polyphenolic moieties was analyzed by soaking the CsNCs-based films in water

(Figure 5B). For shorter incubation times (up to about 40 min), a comparable release profile was detected for all films. Contrarily, for higher incubation times different trends emerged. In the case of CsNCs-E, the concentration of EGCG in the aqueous medium apparently decreased after reaching a maximum equal to about 4.5% of the entrapped polyphenol, while for both TAN and MIHLS, an initial fast release was followed by a much slower release rate. To further investigate the release kinetics and mechanism of the polyphenolic additives for the CsNCs-T and CsNCs-L samples, two models have been considered: Higuchi and Korsmeyer–Peppas. Specifically, the Higuchi model was used to fit the experimental data to evidence the steps of release, while the Korsmeyer–Peppas model was employed to elucidate its mechanism.

The Higuchi model, in its simplified form, can be defined as follows:[38]

$$M_t/M_\infty = K_H \times t^{1/2} \quad (1)$$

where M_t and M_∞ represent the amount of additive released at time t and infinite time, respectively, and K_H is a kinetic constant. The fitting of the experimental data shows for both samples a two-step release (Figure S4A, Supporting Information) characterized by a decrease of the kinetic constants (Table S5, Supporting Information) from the first to the second stage. It can be hypothesized that the first step represents the boundary diffusion from the film surface to the bulk of the solution, while the second is the diffusion of the polyphenol from the bulk of the film to the film surface.[39] By comparing the K_H values of the two samples, it can be noticed that the release rate is faster in the case of TAN with respect to MIHLS, probably due to the much larger size of this latter, while in the second step comparable K_H values have been calculated, suggesting that the interactions occurring between the CsNCs and the polyphenolic additives play the major role in determining the release rate. As to the mechanism of release, the Korsmeyer–Peppas model is expressed as:[40]

$$M_t/M_\infty = K_{KP} \times t^n \quad (2)$$

where K_{KP} is a constant that includes the characteristics of the system and n is the release exponent, which defines the release mechanism. There are two special cases: $n = 0.5$ and $n = 1.0$, respectively indicating diffusion-controlled and swelling-controlled release.[41] Additionally, for $0.5 < n < 1.0$, both phenomena occur simultaneously,[41] and values of n lower than 0.5 denote hindered Fickian diffusion.[42] By applying the model to the experimental data, n equal to 0.15 and 0.29 were respectively found for CsNCs-T and CsNCs-L, highlighting systems characterized by diffusive regime with hampered release, further confirming the presence of intermolecular forces between the polyphenolic molecules and the CsNCs matrix.

On the other hand, to explain the different release trends observed for EGCG, its instability in aqueous media should be taken into consideration, this last following two major degradation pathways, namely epimerization and auto-oxidation.[43] Specifically, in aqueous environments with pH < 5.5, temperature > 50 °C, and for concentrations higher than 10 mmol L^{-1}, the epimerization rate of EGCG into gallocatechingallate is significant.[43] Conversely, the auto-oxidation reaction occurs mainly for pH > 5.5 and consists in the transformation of EGCG into the asinensin A, essentially a dimer of EGCG.[44] This reaction is accompanied by a color change of the solution from pale pink to brown. Since the release tests were carried out at room temperature in water and EGCG concentrations lower than 10 mmol L^{-1} were reached, it can be inferred that the auto-oxidation reaction plays a major role in determining the apparent decrease of the EGCG concentration. It is important to mention that some biological effects have been directly attributed to EGCG degradation products, rather than to EGCG itself,[43] and that the product of epimerization, gallocatechingallate, has been described as showing the same biological properties of the parent molecule.[45]

Polyphenols are well known for their several biological activities like antioxidant and antimicrobial action. The antioxidant activity of natural polyphenols is long known.[46] It is strictly correlated with their structural conformation and the concentration of phenolic groups. Also chitin, chitosan, and their derivatives possess well-documented antioxidant capacity.[47,48]

The potential of the CsNCs-based samples to inhibit free radical species was analyzed by soaking the films into a DPPH-containing solution and measuring its inhibition over time. The data, reported in Figure 5C, evidence in all cases of good antioxidant capacity. Among the tested specimens, CsNCs-G showed lower activity, reaching 50% of inhibition after 135 min. A comparable trend was observed for CsNCs-L, while the tannin-containing samples, i.e., CsNCs-E and CsNCs-T, displayed higher activity, as the 50% of inhibition was achieved after 65 and 30 min, respectively. The results can be explained considering that the antioxidant activity is mainly related to the presence of catechol moieties (EGCG, TAN) and only partially to the presence of simple phenolic groups in the polyphenolic network (MIHLS) (Table S3, Supporting Information). On the other hand, the different molecular weight of the two tannins plays a key role in determining the behavior of CsNCs-E and CsNCs-T. It has been indeed reported that the higher the molecular weight and the concentration of galloyl groups, the greater the free radical scavenging ability,[49] thus the stronger response of the TAN-containing sample, CsNCs-T.

The bactericidal properties of the nanostructured films were tested against Gram-negative (*E. coli*) and Gram-positive (*S. aureus*) strains and determined by measuring the value of antibacterial activity (R), which is calculated as the difference between the CFU found in the CsNCs-based samples and in the control (LDPE sheet) after incubation in the presence of bacterial cells. Values of $R < 1.0$, $1.0 \leq R \leq 2.0$, $2.0 \leq R \leq 3.0$, and $R \geq 3$, respectively indicate a reduction of < 90% (poor activity), 90–99% (satisfactory), 99–99.9% (good) and > 99.9% (very good) viable bacteria.[50] The results are collected in Figure 5D, while Figure S5 (Supporting Information) shows representative photographs of the bacterial colonies grown on agar plates after the incubation in the presence of the CsNCs-based films.

Generally, a higher activity against Gram-positive bacteria was detected. These data are in good agreement with the literature, as a stronger bactericidal effect on Gram-positive than Gram-negative bacteria has been reported for chitosan[51] as well as for natural polyphenols.[52,53] More specifically, satisfactory (*E. coli*) to good (*S. aureus*) activity was measured for the CsNCs-G, confirming the ability of chitosan-based materials to inhibit bacterial growth. As reported in the literature, the mechanism of

action of chitosan is related to the positive charged amino groups that destroy the integrity of the outer membrane of bacteria cells by interacting with its negative charges. Conversely, for pH values higher than the pKa of the amino groups, the activity is due to their ability of chelating the divalent cations of the cellular membrane.[54,55] The high surface area of the nanosized CsNCs, together with the high concentration of surface amino groups, may increase the interaction with the bacterial membrane, further enhancing the bactericidal effect.[54] The introduction of tannins into the CsNCs formulation resulted in a significant increment of the bactericidal behavior of the films, as more than 99.99% (R values > 4) of the *S. aureus* cells were killed after the incubation with CsNCs-E and CsNCs-T films (Figure 5D). Additionally, CsNCs-E highlighted a very good antimicrobial effect also against *E. coli*, while CsNCs-T demonstrated similar behavior to CsNCs-G, suggesting that the presence of tannic acid did not exert any additional effects in this respect. According to the literature, the antimicrobial activity of tannins is due to their complexing ability that results in the damaging of the external bacterial membrane, inhibiting its proper functioning.[56] Furthermore, a certain dependence of the activity from the molecular weight and flexibility of these molecules has been reported.[57]

Lastly, the CsNCs-L film displayed only poor antimicrobial activity, as R values < 1 were recorded (Figure 5D). To better explain this behavior it has to be considered that the concentration of released MIHLS is low (in the range of μg mL^{-1}, Figure 5B), while minimum inhibition concentration values in the mg mL^{-1} order of magnitude were reported for various lignin samples both against Gram-positive and Gram-negative bacteria.[53] Moreover, the interaction of the sulfonate groups with the amino functionalities of CsNCs may have decreased the overall film activity, which was found lower than the CsNCs-G sample.

3. Conclusion

In this work, free-standing, easily handleable, fully biobased films have been fabricated from CsNCs via a simple and straightforward methodology. The film characteristics were modulated by introducing three water-soluble natural polyphenols, whose molecular weight and content of hydroxy groups played a major role in this respect. Both EGCG and TA contain a high amount of phenolic and catecholic OH groups, but differ in terms of molecular weight, the first having a monomeric structure, while the second being a highly branched oligomer. On the other hand, MIHLS contains a significant amount of aliphatic OH groups and a much lower amount of phenolics but displays higher molecular weight with respect to the other compounds. Therefore, EGCG and TA may form a greater hydrogen bonding network but involving CsNCs that are closer to the polyphenol itself. On the other hand, MIHLS can generate a smaller number of interactions, yet at a longer range. These features significantly affect the physic–mechanical properties of the films, as the presence of the polyphenols resulted in an increase of the elastic modulus and a reduction of the water absorption of CsNCs-E, CsNCs-T, and CsNCs-L with respect to CsNCs-G. They indeed act as crosslinking agents due to the formation of non-covalent interactions with the CsNCs, by respectively reinforcing the nanocrystal-based matrix and hampering the film swelling. Of note, due to the high concentration of polar functional groups, the surface wettability is not significantly affected, rather a slight increment of water contact angle was measured for CsNCs-L due to the aromatic hydrophobic backbone. Interestingly, all the materials preserve high transparency and flexibility.

In addition, the presence of tannins also allowed to enhance the functional features of the CsNCs-G film. CsNCs-E and CsNCs-T displayed powerful radical scavenging and antimicrobial activity. CsNCs-E especially highlighted a bactericidal effect as high as 99.99% against both Gram-negative (*E. coli*) and Gram-positive (*S. aureus*) bacterial strains. Also, in this case, the chemical structure of the additives is a key factor. Antioxidant and antibacterial capacity are linked to the catechol content of the polyphenolic species and to their release rate, this last in turn influenced by the interactions of these molecules with the CsNCs matrix, as kinetics studies determined a hindered Fickian diffusion. Smaller molecules rich in phenolics (EGCG) exerted a strong action, while in the case of larger molecules depleted of OH functionalities (MIHLS) the activity was comparable or inferior to the polyphenol-free film.

Therefore, the study demonstrates that the film-forming ability of surface-deacetylated chitin nanocrystals, together with the formation of a hydrogen bond network brought by the introduction of natural polyphenolic molecules, can be exploited on macroscale level to develop of bioactive materials with promising tensile and functional properties that could be exploited for biomedical or packaging applications.

In conclusion, this work presented an upcycling process that leads to completely biobased, innovative active films from largely available biomass residues in full compliance with the circular economy paradigms, thus opening up new exploitation routes for a very peculiar, yet underutilized resource as chitin.

4. Experimental Section

Materials: Chitin from shrimp shells (Sigma Aldrich, practical grade) in the form of flakes was used as the starting material for the preparation of ChNCs. Hardwood lignosulfonate (Borregaard LignoTech), Epigallocatechin gallate (Galeno, 95%), and tannic acid (Sigma Aldrich, ACS reagent grade) were used as additives.

Dimethyl sulfoxide (HPLC grade, ≥ 99%), methanol (≥ 99.8%), hydrochloric acid (37%), lithium chloride (≥ 99%), sodium hydroxide (≥ 98%), potassium bromide (FT-IR grade), 2-chloro-4,4,5,5-tetramethyl-1,3,2-dioxaphospholane (95%), cholesterol (≥ 99%), chromium(III) acetylacetonate (≥ 97%), pyridine (99.8%), sulphanilamide (≥ 99%) and tungsten(VI) oxide powder (99.9%) were purchased from Sigma Aldrich, while acetic acid (99.0%) and glycerol (≥ 99%) from VWR.

Ultrapure water (Millipore-Milli-Q Water System) was employed unless otherwise stated.

Preparation of Chitin Nanocrystals (ChNCs): The synthesis of ChNCs was carried out as previously reported with minor modifications.[15] Specifically, chitin flakes at a concentration of 35 mg mL^{-1} were dispersed in a 3 mol L^{-1} HCl solution in a round bottom flask. The reaction mixture was maintained under mechanical stirring at reflux for 4 h. Subsequently, the mixture was cooled to room temperature, the solid was recovered by centrifugation (4700 *g*, 15 min) and washed with deionized water. The washing/centrifugation steps were repeated three times. The recovered precipitate was then re-suspended in deionized water and sonicated at 40% amplitude for 10 min using a Branson Digital Sonifier (Model 450L, Ultrasonic Corporation) equipped with a 20 KHz Branson probe ending in a horn tip (max amplitude 160 W) to obtain an opalescent colloidal suspension. After the sonication step, the mixture was diluted with

1 L of deionized water and a 1 mol L^{-1} NaOH solution was added to induce the precipitation of the ChNCs. Finally, the ChNCs were subjected to washing/centrifugation cycles (see above) until neutral pH. The amount of ChNCs in the never-dried gel was determined gravimetrically by drying the sample at 100 °C under vacuum to constant weight.

Preparation of Surface Deacetylated Chitin Nanocrystals (CsNCs): A literature protocol was employed to obtain CsNCs, with minor modifications.[15] Briefly, ChNCs were dispersed in a 12.5 mol L^{-1} NaOH solution at a concentration of 16 mg mL^{-1}. The reaction was carried out under reflux and mechanical stirring for 12 h. The reaction mixture was cooled to room temperature and the solid was recovered by centrifugation (4700 *g*, 15 min). CsNCs were subjected to washing/centrifugation cycles (see above) until neutral pH. The amount of CsNCs in the never-dried gel was determined gravimetrically as described above.

Characterization of Nanocrystals—Elemental Analysis: The chemical composition of the starting chitin and of the produced ChNCs and CsNCs was evaluated by CHNS analysis. An elemental Elemental UNICUBE instrument was used for the measurements. The degree of deacetylation (D_D) was calculated according to the following formula, as previously reported in the literature:[58]

$$D_D = 100 \times \left(4 - 0.583093 \times W_{C/N}\right) \quad (3)$$

where $W_{C/N}$ = mass of carbon / mass of nitrogen.

Characterization of Nanocrystals—Fourier-Transform Infrared Spectroscopy (FT-IR): FT-IR spectra were recorded on potassium bromide (KBr) discs (16 scans), in the spectral range 4000–400 cm^{-1} using a Perkin Elmer Spectrum One spectrophotometer. Prior to the analysis, the samples were dried at 100 °C to constant weight.

Characterization of Nanocrystals—Thermogravimetric Analysis (TGA): TGA analysis was performed with a Perkin Elmer TGA 4000 under inert atmosphere (nitrogen, flow rate 20 mL min^{-1}), and a heating rate of 10 °C min^{-1} in the range of 50–800 °C.

Characterization of Nanocrystals—Dynamic Light Scattering (DLS) and Zeta Potential: To evaluate the size and surface charge of the nanocrystals, DLS and zeta potential analyses were carried out on a Malvern Zetasizer Ultra. Prior to the analysis, each sample was suspended at a concentration of 1 mg mL^{-1} in an aqueous solution at pH 4.0.

Characterization of Nanocrystals—Atomic Force Microscopy (AFM): The analysis was carried out on a Park XE-7 (Park Systems Inc.) instrument coupled with SmartScan software. Sample preparation consisted of the deposition of a drop of nanocrystals dispersion (10 µL) on a mica support and then, after 15 s, in the removal of the non-absorbed material by immersing the sample in water for an additional 15 s. Prior to the analysis, the samples were dried at room temperature.

Preparation of the Methanol Insoluble Fraction of Hardwood Lignosulfonate (MIHLS): Due to the high structural heterogeneity and molecular dispersity of technical lignins, MIHLS was chosen with the aim of isolating a purer, more homogeneous and higher molecular weight cut of the material yet preserving the desired water solubility. MIHLS was obtained as previously reported in the literature,[59] with minor modifications. Briefly, the fractionation was carried out by suspending 5 g of lignosulfonate powder into 250 m of methanol. The mixture was stirred at room temperature for 20 h. The MIHLS was then collected by centrifugation (4700 *g*, 20 min) and dried under vacuum at 40 °C to constant weight.

Preparation of the Methanol Insoluble Fraction of Hardwood Lignosulfonate (MIHLS)—Molecular Weight Determination: The molecular weight of MIHLS was determined by gel permeation chromatography (GPC) operated on a Shimadzu HPLC system by employing a Plgel 5 µm MiniMIX-C column (250 × 4.6 mm). HPLC-grade DMSO containing 0.1% lithium chloride was used as eluent (0.2 mL min^{-1}, 70 °C). Calibration was performed with polystyrene sulfonate standards (Sigma Aldrich, M_w range 4.3–2600 kDa) and lignin model compounds (330–640 Da). The samples were dissolved in HPLC-grade DMSO and filtered through a 0.2 µm syringe filter prior to injection.

Preparation of the Methanol Insoluble Fraction of Hardwood Lignosulfonate (MIHLS)—Quantification of the Hydroxyl Groups Content: The concentration of hydroxyl groups in the polyphenols was determined by ^{31}P-NMR spectroscopy. A Bruker 400 MHz NMR spectrometer was used for the analyses. The sample (previously dried to constant weight and accurately weighed) was phosphitylated with the use of 2-chloro-4,4,5,5-tetramethyl-1,3,2-dioxaphospholane, as previously reported in the literature.[60] A mixture of deuterated chloroform and anhydrous pyridine in a volume ratio 1:1.6 was used as a solvent and cholesterol was used as an internal standard.

Fabrication of CsNCs-Based Films: Free-standing films of CsNCs were obtained by solvent-casting. CsNCs were first dispersed in deionized water at a concentration of 35 mg mL^{-1} and then a 1.6 mol L^{-1} acetic acid solution was added to reach a final pH of 5.7. The mixture was placed in an ultrasonic bath for 15 min at 40 °C (Soltec Sonica ultrasonic cleaner) to aid the formation of a colloidal suspension. Glycerol was added to the formulation as a plasticizer at 30% w/w_{CsNCs} to obtain the CsNCs-G film. Epigallocatechin gallate, tannic acid or the methanol insoluble fraction of hardwood lignosulphonate were also introduced in the formulation at 1% w/w_{CsNCs} to yield the CsNCs-E, CsNCs-T and CsNCs-L films, respectively.

The suspension was then poured into circular silicon molds (4.5 cm of diameter) and dried at room temperature.

Characterization of CsNCs-Based Films—Film Thickness: The thickness of the films was determined using a handheld digital micrometer with a sensitivity of ± 0.1 µm.

Characterization of CsNCs-Based Films—Color Determination: The color analysis was carried out in accordance with the CIELAB system by means of a Konica Minolta Colorimeter CM-2500d with an illuminant D65. The parameters such as L* (lightness), a* (redness/greenness), and b* (yellowness/blueness) were determined using the instrument software. The reported values represent the average of at least five readings performed in different film areas.

The total color difference (ΔE) was calculated as follows:

$$\Delta E = \left[(\Delta L*)^2 + (\Delta a*)^2 + (\Delta b*^2)\right]^{1/2} \quad (4)$$

where ΔL*, Δa*, and Δb* represent the difference between the color parameters of the standard sample (CsNCs-G) and those of the film containing the polyphenolic compound.

For each film, also HUE, CHROMA, and opacity were determined.

HUE, which represents the color, is equal to:

$$HUE = arctan\,(b*/a*) \quad (5)$$

when both a* and b* take positive values, and to:

$$HUE = 180 + arctan\,(b*/a*) \quad (6)$$

when a* is negative and b* is positive.[61]

CHROMA, that describes the strength of the color, was obtained from:

$$\text{CHROMA} = \left[(a*)^2 + (b*^2)\right]^{1/2} \quad (7)$$

Lastly, the opacity was measured by the following formula, as previously reported:[62]

$$\text{Opacity} = A_{600}/t \quad (8)$$

where A_{600} is the absorbance value at 600 nm wavelength, measured using a Shimadzu UV-1800 UV/Visible Scanning Spectrophotometer, and t is the film thickness.

Characterization of CsNCs-Based Films—Scanning Electron Microscopy (SEM): A Zeiss Sigma Field Emission Scanning Electron Microscope (FE-SEM) was used for the analysis. Micrographs of the films' surface were acquired on non-sputtered samples at 1 kV with an InLens detector.

Characterization of CsNCs-Based Films—Water Contact Angle: The water contact angle (WCA) measurements were carried out on a First Ten Angstroms (FTA) 1000 Drop Shape instrument at room temperature. The

WCA was calculated by analyzing the side profile of a deionized water drop (6 µL) placed on the film surface after 1 s from deposition. At least ten drops deposited on different areas of each film were analyzed. WCA are reported as the average value ± standard deviation. The water absorption kinetics were evaluated by measuring the static contact angle over a time frame of 5 min.

Characterization of CsNCs-Based Films—Water Absorption: The amount of water absorbed by the films was calculated gravimetrically. Prior to the analysis, each film was dried in a static oven at 30 °C under vacuum to constant weight and its dry weight was determined. The film was subsequently soaked in deionized water and placed in an ArgoLab Ski4 shaker at room temperature under stirring (150 rpm). After 10 min the films were withdrawn, gently wiped with Kimtech paper, and weighed. The percentage of absorbed water (W_{ab}) was calculated according to the following formula:

$$W_{ab} = 100 \times (w_{10} - w_0)/(w_0) \quad (9)$$

where w_{10} is the weight of the film after 10 mins of incubation in water and w_0 is the weight of the dry film.

The size (length and width) and thickness of the films were measured before and after incubation.

Characterization of CsNCs-Based Films—Tensile Tests: Stress–strain measurements were performed on rectangular films (5 mm wide and 0.05 mm thick) using an MTS Insight moving beam dynamometer machine equipped with a 100 N load cell. The gauge length was equal to 20 mm and the crosshead speed was set to 0.5 mm s^{-1}. The elastic modulus (E) was determined from the first linear segment of the stress–strain curve. At least five replicates were run for each sample and the results were provided as the average ± standard deviation.

Characterization of CsNCs-Based Films—Release of Polyphenols in Water: Polyphenol-containing CsNCs films (CsNCs-E, CsNCs-T, and CsNCs-L) of 4 cm^2 in size were soaked in ultrapure water and placed in an ArgoLab Ski4 shaker at 37 °C under stirring (150 rpm). Aliquots of the supernatant were withdrawn at predetermined time intervals over a time span of 5 days and analyzed using a Shimadzu UV-1800 UV/Visible Scanning Spectrophotometer to evaluate the amount of polyphenol released in the medium. For each polyphenol, a calibration curve was constructed in the concentration range of 0.0025–0.02 mg mL^{-1}.

Characterization of CsNCs-Based Films—Antioxidant Activity: The antioxidant activity was assessed by measuring the free radical scavenging effect on 1,1-diphenyl-2-picrylhydrazyl (DPPH). Rectangular film specimens (4 cm^2) of about 10 mg in weight were soaked in a vial containing 2 mL of a 6×10^{-5} mol L^{-1} ethanol solution of DPPH and placed in a ArgoLab Ski4 shaker at 150 rpm and 25 °C. At specific time intervals, the absorbance at 517 nm was measured by means of a Shimadzu UV-1800 UV/Visible Scanning Spectrophotometer against a control (DPPH solution in the absence of the film). Each test was carried out in triplicate. The results are expressed as the percentage of inhibition of the DPPH radical, calculated according to the following equation:

$$\text{Radical scavenging ability } (\%) = (1 - A_S/A_C) \times 100 \quad (10)$$

where A_s is the absorbance of the DPPH solution containing the film sample and A_c is the absorbance of the DPPH solution without the film.

Characterization of CsNCs-Based Films—Antibacterial Activity: The antibacterial activity of the films was determined against *E. coli* and *S. aureus* in accordance with the ISO 22196:2011 protocol. The inoculum of bacterial strains was prepared from fresh overnight culture in LB broth. A final bacterial concentration of 1×10^5 CFU mL^{-1} was used for the test. All films were sterilized by UV irradiation (30 mins each side) prior to testing. 300 µL of the cell suspension were placed between the sample film (15.9 cm^2) and an LDPE sheet (previously sterilized) and incubated in sterile Petri dishes at 37 °C in upward of 90% humidity for 24 h. Negative (no bacterial inoculum) and positive (inoculum in between two LDPE sheets) controls were incubated under the same conditions.

At the end of the incubation, 3 mL of fresh LB broth was added to each Petri dish for the detachment and resuspension of the bacteria, and the Petri were shaken at 250 rpm for 180 s. Afterward, six-fold dilutions were made and the samples were cultured via drop (10 µL) plate method (37 °C, 24 h). Subsequently, the colony-forming units (CFU) were counted and the antibacterial activity (R) was determined as follows:[50]

$$R = Ut - At \quad (11)$$

where R is the difference between the $\log_{10}$ of the average CFU number on the reference samples (Ut) and the $\log_{10}$ of the average CFU number on the test samples (At).

Supporting Information

Supporting Information is available from the Wiley Online Library or from the author.

Acknowledgements

Open access publishing facilitated by Universita Ca' Foscari, as part of the Wiley - CRUI-CARE agreement.

Conflict of Interest

Daniele Massari, Matteo Gigli, Claudia Crestini have patent pending to Ca' Foscari University of Venice and University of Pavia.

Author Contributions

D.M. performed investigation, data curation, validation, and methodology; M.S. performed methodology, validation, and supervised the project and wrote, reviewed, and edited the final manuscript; M.G. performed data curation, validation, project administration, formal analysis, conceptualized, and supervised the project and acquired funds and resources, wrote the original draft, and wrote, reviewed and edited the final manuscript; C.C. conceptualized, acquired funds and resources, did project administration, and wrote, reviewed and edited the final manuscript.

Data Availability Statement

The data that support the findings of this study are available from the corresponding author upon reasonable request.

Keywords

antimicrobial properties, antioxidant activity, biobased films, chitin nanocrystals, chitosan nanocrystals, natural polyphenols

Received: June 3, 2024
Revised: August 21, 2024
Published online: September 13, 2024

[1] C. Xu, M. Nasrollahzadeh, M. Selva, Z. Issaabadi, R. Luque, *Chem. Soc. Rev.* **2019**, *48*, 4791.
[2] T. Maschmeyer, R. Luque, M. Selva, *Chem. Soc. Rev.* **2020**,*49*, 4527.
[3] S. Kaur, G. S. Dhillon, *Crit. Rev. Biotechnol.* **2015**, *35*, 452744.
[4] J. Wattjes, A. Niehues, S. Cord-Landwehr, J. Hoßbach, L. David, T. Delair, B. M. Moerschbacher, *J. Am. Chem. Soc.* **2019**, *141*, 3137.

[5] M. Rinaudo, *Prog. Polym. Sci.* **2006**, *31*, 603.
[6] M. Ali, M. J. Bathaei, E. Istif, S. N. Karimi, L. Beker, *Adv. Healthcare Mater.* **2023**, *12*, e2300318.
[7] W. Suginta, P. Khunkaewla, A. Schulte, *Chem. Rev.* **2013**, *10*, 5458.
[8] R. Vinodh, Y. Sasikumar, H. J. Kim, R. Atchudan, M. Yi, *J Ind Eng Chem* **2021**, *104*, 155.
[9] I. Younes, M. Rinaudo, *Mar Drugs* **2015**, *13*, 1551133.
[10] R. Kumari, M. Kumar, V. Vivekanand, N. Pareek, *Renew Sustain Energy Rev* **2023**, *184*, 113595.
[11] J. Wattjes, S. Sreekumar, C. Richter, S. Cord-Landwehr, R. Singh, N. E. El Gueddari, B. M. Moerschbacher, *Reac. Funct. Polym.* **2020**, *151*, 104583.
[12] T. Jin, T. Liu, E. Lam, A. Moores, *Nanoscale Horiz.* **2021**, *6*, 505.
[13] S. Lee, L. T. Hao, J. Park, D. X. Oh, D. S. Hwang, *Adv. Mater.* **2023**, *35*, 2203325.
[14] Y. Luo, Y. Li, K. Liu, L. Li, W. Wen, S. Ding, Y. Huang, M. Liu, C. Zhou, B. Luo, *Biomacromolecules* **2023**, *12*, 2942.
[15] A. G. Pereira, E. C. Muniz, Y. L. Hsieh, *Carbohydr. Polym.* **2014**, *107*, 158.
[16] Y. Liu, M. Liu, S. Yang, B. Luo, C. Zhou, *ACS Sustainable Chem. Eng.* **2018**, *6*, 325.
[17] A. G. Pereira, C. S. Nunes, A. F. Rubira, E. C. Muniz, A. R. Fajardo, *Carbohydr. Polym.* **2021**, *266*, 118116.
[18] A. Narkevicius, L. M. Steiner, R. M. Parker, Y. Ogawa, B. Frka-Petesic, S. Vignolini, *Biomacromolecules* **2019**, *20*, 1582830.
[19] Y. Fan, H. Fukuzumi, T. Saito, A. Isogai, *Int. J. Biol. Macromol.* **2012**, *50*, 69.
[20] J. Chen, Z. Ling, X. Wang, X. Ping, Y. Xie, H. Ma, J. Guo, Q. Yong, *Chem. Eng.* **2023**, *466*, 143148.
[21] Z. Ling, J. Chen, X. Wang, L. Shao, C. Wang, S. Chen, J. Guo, Q. Yong, *Carbohydr. Polym.* **2022**, *296*, 119920.
[22] J. Chen, Y. Ren, W. Liu, T. Wang, F. Chen, Z. Ling, Q. Yong, *Int. J. Biol. Macromol.* **2021**, *193*, 1324.
[23] Z. Ling, W. Liu, Y. Ren, H. Chen, C. Huang, C. Lai, Q. Yong, *Carbohydr. Polym.* **2021**, *270*, 118328.
[24] X. Li, J. Li, X. Shen, M. Cao, Y. Wang, W. Zhang, Y. Xu, Z. Ling, S. Chen, F. Xu, *ACS Sustainable Chem. Eng.* **2024**, *12*, 5427.
[25] T. D. Nguyen, B. U. Peres, R. M. Carvalho, M. J. MacLachlan, *Adv. Funct. Mater.* **2016**, *26*, 2875.
[26] J. D. Goodrich, W. T. Winter, *Biomacromolecules* **2007**, *8*, 252.
[27] F. Larbi, A. García, L. J. Del Valle, A. Hamou, J. Puiggalí, N. Belgacem, J. Bras, *Carbohydr. Polym.* **2018**, *196*, 385.
[28] C. Peng, G. Chen, *Materials* **2018**, *11*, 1883.
[29] A. G. Pereira, E. C. Muniz, Y. L. Hsieh, *Carbohydr. Polym.* **2015**, *123*, 46.
[30] P. Das, M. K. Das, in *Nanocosmeceuticals*, Academic Press, Cambridge, Massachusetts **2022**, p. 95.
[31] S. A. Jin, R. J. Spontak, *Adv. Ind. Eng. Polym. Res.* **2023**, *6*, 356.
[32] W. Li, W. Liu, W. Wen, H. Liu, M. Liu, C. Zhou, B. Luo, *Carbohydr. Polym.* **2019**, *209*, 92.
[33] M. Xu, W. Li, C. Ma, H. Yu, Y. Wu, Y. Wang, Z. Chen, J. Li, S. Liu, *J Mater Chem* **2018**, *6*, 5391.
[34] J. Wang, W. Chen, T. Dong, H. Wang, S. Si, X. Li, *Green Chem.* **2021**, *23*, 10062.
[35] L. A. Van den Broek, R. J. Knoop, F. H. Kappen, C. G. Boeriu, *Carbohydr. Polym.* **2015**, *116*, 237.
[36] C. F. João, C. Echeverria, A. Velhinho, J. C. Silva, M. H. Godinho, J. P. Borges, *Carbohydr. Polym.* **2017**, *155*, 372.
[37] Z. Ling, Q. Gu, Y. Tan, M. Yan, H. Dong, L. Shao, S. Chen, Y. Xu, C. Lu, Q. Yong, *Int. J. Biol. Macromol.* **2024**, *261*, 129859.
[38] T. Higuchi, *J. Pharm. Sci.* **1963**, *52*, 1145.
[39] Y. Huang, X. Lee, M. Grattieri, F. C. Macazo, R. Cai, S. D. Minteer, *J. Mater. Sci.* **2018**, *53*, 12641.
[40] R. W. Korsmeyer, R. Gurny, E. Doelker, P. Buri, N. A. Peppas, *Int. J. Pharm.* **1983**, *15*, 25.
[41] M. L. Bruschi, *Strategies to Modify the Drug Release from Pharmaceutical Systems*, Woodhead Publishing, Sawston, United Kingdom **2015**, pp. 63–86.
[42] M. Fosca, J. V. Rau, V. Uskoković, *Bioact Mater* **2021**, *7*, 341.
[43] O. Krupkova, S. J. Ferguson, K. Wuertz-Kozak, *J. Nutr. Biochem.* **2016**, *37*, 1.
[44] Z. Hou, S. Sang, H. You, M. J. Lee, J. Hong, K. V. Chin, C. S. Yang, *Cancer Res.* **2005**, *65*, 8049.
[45] J. Alfke, U. Kampermann, S. P. Kalinina, M. Esselen, *Eur. Food Res. Technol.* **2021**, *247*, 2961.
[46] X. Lu, X. Gu, Y. Shi, *Int. J. Biol. Macromol.* **2022**, *210*, 716.
[47] D. H. Ngo, S. K. Kim, *Adv. Food Nutr. Res.* **2014**, *73*, 15.
[48] H. Tomida, T. Fujii, N. Furutani, A. Michihara, T. Yasufuku, K. Akasaki, T. Maruyama, M. Otagiri, J. M. Gebicki, M. Anraku, *Carbohydr. Res.* **2009**, *344*, 1690.
[49] T. Yokozawa, C. P. Chen, E. Dong, T. Tanaka, G. I. Nonaka, I. Nishioka, *Biochem. Pharmacol.* **1998**, *56*, 213.
[50] A. Richert, E. Olewnik-Kruszkowska, G. B. Dąbrowska, H. P. Dąbrowski, *Int. J. Mol. Sci.* **2022**, *23*, 268.
[51] J. Li, S. Zhuang, *Eur. Polym. J.* **2020**, *138*, 109984.
[52] B. Kaczmarek, *Materials (Basel)* **2020**, *13*, 3224.
[53] I. Ullah, Z. Chen, Y. Xiea, S. S. Khan, S. Singh, C. Yu, G. Cheng, *Int. J. Biol. Macromol.* **2022**, *208*, 819.
[54] A. G. Pereira, A. R. Fajardo, A. P. Gerola, J. H. S. Rodrigues, C. V. Nakamura, E. C. Muniz, Y. L. Hsieh, *Carbohydr. Polym.* **2020**, *250*, 116954.
[55] Y. Qin, S. Zhang, J. Yu, J. Yang, L. Xiong, Q. Sun, *Carbohydr. Polym.* **2016**, *147*, 372.
[56] E. Olchowik-Grabarek, S. Sękowski, A. Kwiatek, J. Płaczkiewicz, N. Abdulladjanova, V. Shlyonsky, I. Swiecicka, M. Zamaraeva, *Membranes (Basel)* **2022**, *12*, 1124
[57] E. Olchowik-Grabarek, S. Sekowski, M. Bitiucki, I. Dobrzynska, V. Shlyonsky, M. Ionov, P. Burzynski, A. Roszkowska, I. Swiecicka, N. Abdulladjanova, M. Zamaraeva, *Sci. Rep.* **2020**, *10*, 11168.
[58] Z. M. Dos Santos, A. L. P. F. Caroni, M. R. Pereira, D. R. da Silva, J. L. C. Fonseca, *Carbohydr. Res.* **2009**, *344*, 2591.
[59] M. Sgarzi, M. Gigli, C. Giuriato, C. Crestini, *Materials* **2022**, *15*, 1857.
[60] D. S. Argyropoulos, N. Pajer, C. Crestini, *J Vis Exp* **2021**, *2*, e62696.
[61] M. R. McLellan, L. R. Lind, R. W. Kime, *J Food Qual* **1995**, *18*, 235.
[62] S. Bhatia, A. Al-Harrasi, M. Jawad, Y. A. Shah, M. S. Al-Azri, S. Ullah, M. K. Anwer, M. F. Aldawsari, E. Koca, L. Y. Aydemir, *Biomimetics* **2023**, *8*, 172.